

RSC Advances



This is an *Accepted Manuscript*, which has been through the Royal Society of Chemistry peer review process and has been accepted for publication.

Accepted Manuscripts are published online shortly after acceptance, before technical editing, formatting and proof reading. Using this free service, authors can make their results available to the community, in citable form, before we publish the edited article. This *Accepted Manuscript* will be replaced by the edited, formatted and paginated article as soon as this is available.

You can find more information about *Accepted Manuscripts* in the [Information for Authors](#).

Please note that technical editing may introduce minor changes to the text and/or graphics, which may alter content. The journal's standard [Terms & Conditions](#) and the [Ethical guidelines](#) still apply. In no event shall the Royal Society of Chemistry be held responsible for any errors or omissions in this *Accepted Manuscript* or any consequences arising from the use of any information it contains.



Surface Molecularly Imprinted Electrochemical sensor for Phenol based on SiO₂ nanoparticles

Gaixia Zhang,^a Li Fang*,^a Feifei Li^a and Baojiao Gao^b

A novel surface molecularly imprinted electrochemical sensor (MIECS) for recognition and detection of phenol was constructed by dispersing a molecularly imprinted polymer (MIP) film on a multi-walled carbon nanotubes (MWNTs) modified glass carbon electrode (GCE). An adsorption equilibrium of phenol to polyethyleneimine (PEI, grafted to SiO₂ nanoparticles) had been achieved before molecular imprinting was carried out towards PEI by using phenol as a template and ethylene glycol diglycidyl ether (EGDE) as cross-linker. The MIP was fabricated after the removal of phenol and the etching of SiO₂ nanoparticles. The obtained MIP and MIECS were characterized by fourier transform infrared spectroscopy (FT-IR), scanning electron microscope (SEM), cyclic voltammetry (CV) and differential pulse voltammetry (DPV). The sensor exhibited a remarkable enhancement of current response since the charge transfer process had been facilitated by the etching of SiO₂ nanoparticles and the modification of GCE with MWNTs-COOH. The sensor showed specific recognition ability to phenol rather than the other phenolic compounds with an excellent repeatability since the recognition sites were distributed on the surface of the polymer. The linear range of the calibration curve was 1×10^{-8} – 1.8×10^{-6} M with the detection limit of 4.2×10^{-9} M (S/N=3) when potassium ferricyanide was used as the electro-chemical active probe, superior to the other electrochemical sensors reported in literatures. The fabricated sensor exhibited a good performance on the determination of phenol in real samples as well.

Received 00th January 20xx,
Accepted 00th January 20xx

DOI: 10.1039/x0xx00000x

www.rsc.org/

1. Introduction

Phenol is an essential material used for production of various chemicals, such as pesticide, coating, plastics, dyes, etc, and it's also widely applied in petrochemical and coal chemical industry¹. Nevertheless, phenol is classified as one of the priority pollutants by the United States Environmental Protection Agency (USEPA)² due to its strong toxicity to human being, such as cell lesions, protein inactivation, and even leading to death^{3,4}. In the past decades, the

indiscriminate discharge of industrial wastewater containing phenolic substances has caused very serious environmental pollution. In particular, the contamination of drinking water directly threatened the local people's lives. Therefore, the treatment of phenolic wastewater has attracted worldwide concern and has been efficient extensively studied.

One of the premises of treatment of phenolic wastewater is accurately and fast determining the content of phenol in phenolic wastewater. The conventional phenol detecting methods mainly include spectrophotometry (SP)⁵, high performance liquid chromatography (HPLC)⁶, gas chromatography (GC)⁷ etc. Recently, the electrochemical sensors for phenol detection⁸⁻¹⁰ have been rapidly developed because of their high detecting efficiency

^a School of Chemistry and Chemical Engineering, Shanxi University, Taiyuan 030006, PR China, E-mail: Fangli@sxu.edu.cn

^b Department of Chemical engineering, North University of China, Taiyuan 030051, PR China, E-mail: gaobaojiao@126.com.

ARTICLE

RSC Advances

and low cost, nevertheless, poor selectivity and lower sensitivity caused by the interference of other compositions in practical samples hindered the application of electro-analytical methods^{11,12}. Hence, it is of great important and necessity to construct a sensitive and accurate electrochemical sensor with specific recognition for phenol detection.

Molecularly imprinted polymers (MIPs)¹³⁻¹⁵ are a kind of well-tailored smart materials, which are distributed with a great deal of imprinted cavities designed for the target template molecules. The cavities are highly matched with the template molecules in shape, size and functional group arrangement. MIPs can specifically recognize and bind the template molecules due to their memory function to the structure of template molecules¹⁶. Lately MIPs have been applied for recognition, separation, enrichment, analysis and monitoring of matters¹⁷⁻¹⁸, showing structure-activity predetermination, high stability and long lifespan, etc. However, the recognition sites of MIPs synthesized by means of traditional mass polymerization are mostly encapsulated in the bulk of polymer, which inevitably hinder the binding between the imprinted molecules and recognition sites due to the diffusion resistance¹⁹.

Surface molecularly imprinted polymers can solve the above binding problem since their recognition sites are located on the surface of the MIPs²⁰⁻²², though it is still difficult to achieve fast and high-efficiency detection to combine surface molecularly imprinted technology and the regular characterization methods such as SP, HPLC and GC. Electrochemical sensors by far has got much attention due to the advantages including high-efficiency, high sensitivity, speediness, together with easy carrying, easy operation and low cost. Thus, constructing imprinted electrochemical sensors by combining surface imprinted technique with electrochemical technique is one of the extremely important methods to specifically detect the target molecules²³.

Zhao and Hao²⁴ developed a novel electrochemistry-molecular imprinting sensor for tert-butylhydroquinone (TBHQ) detection in foodstuff. In their work, TBHQ-imprinted core-shell nanoparticles (TICSNs) were prepared by polymerization to the silica nanoparticles (SiO₂NPs) modified with (3-chloropropyl) trimethoxysilan and polyethylenimine, respectively, with ethylene glycol dimethacrylate as cross-linker. The fabricated TICSNs-sensor showed a high selective recognition ability and fast response to TBHQ due to the remarkably increased effective binding sites based on their specific surface area. The conductivity of the sensor was very poor though the linear range of the calibration curve was 0.1-50.0 mg kg⁻¹ with the detection limit of 0.27 mg kg⁻¹, which might be caused by the non-conductivity of SiO₂NPs. By electropolymerization, Li *et al*²⁵ deposited polypyrrole on an aldehyde group-functionalized silica (SiO₂-CHO) modified Au electrode to fabricate a three-dimensional macroporous electrochemical sensor for bovine hemoglobin recognition (BHb). The prepared sensor exhibited an excellent selectivity recognition and fast rebinding capacity for BHb since all the cavities were located at the surface of the polymers. With the etching of SiO₂ nanoparticles, both the conductivity and the efficiency of mass transport were increased. Zhou *et al*²⁶ established a multiporous imprinted electrochemical sensor for the detection of epinephrine (EP) by electropolymerization of a polypyrrole film on the surface of SiO₂NPs and multiwalled carbon nanotubes (MWNTs) modified glassy carbon electrode (GCE). In this case, a multiporous network structure was obtained by the etching of SiO₂NPs, leading to the improvement of the rebinding rate and efficiency of imprinted sites of the sensor. Moreover, a remarkably increase of the electrochemical sensitivity was achieved by using MWNTs to modify the GCE electrode. The fabricated sensor showed an excellent selectivity to EP and a good linear range of 3.0×10⁻⁷ M - 1.0×10⁻³ M with a detection limit of 3.0×10⁻⁸ M.

To date, the surface molecularly imprinted electrochemical sensor (MIECS) based on SiO₂ nanoparticles for phenol detection has not yet been reported. In this paper, combining graft polymerization, surface imprinting and electrochemical technique, we fabricated a MIECS for phenol detection. Characterized by cycle voltammetry (CV) and difference pulse voltammetry (DPV), the obtained sensor showed high selectivity and sensitivity to phenol, indicating its potential application for phenol recognition and detection environmentally.

2. Experimental

2.1 Chemicals and reagents

The main chemicals and reagents used in this research are as follows: silica nanoparticles (20nm, Qingdao Haiyang chemical Co., Ltd), dimethylbenzene (Sinopharm Chemical Reagent Co., Ltd), γ -chloropropyl trimethoxy siloxane (CP-TMS, 99%, Qufu Wand Chemical Co., Ltd.), polyethyleneimine (PEI, 50 wt.%, Wuhan Qianglong New Chemical Materials Co. Ltd.), ethylene glycol diglycidyl ether (EGDE, Wuxi City Fangrong Material Co., Ltd), multi-walled carbon nanotubes (MWNTs, 95%, Shenzhen Nanotech Port Co., Ltd).

2.2 Preparation of MIP

The MIP@SiO₂ was fabricated according to reference²⁷⁻²⁹. Firstly, 20 g of as-received SiO₂ was activated by 5% HCl, the activated SiO₂ were then added into dimethylbenzene containing CP-TMS and refluxed with stirring at 80 °C for 6h. Secondly, 1 g of chloropropylation of SiO₂ and 50 mL of PEI (50 wt. %) were mixed and refluxed at 90 °C with stirring for 5 h. The product was washed with ultrapure water and then centrifuged followed with vacuum drying at 40 °C, labeled as PEI/SiO₂. Afterwards, PEI/SiO₂ was immersed in 500 mL of phenol aqueous solution (1 g/L) and kept for 8 hours to reach an adsorption equilibrium³⁰. Finally, The PEI/SiO₂

saturated with phenol was added into 100 mL of the solution of absolute ethanol with 5 mL of EGDE, the reaction was carried out for 8h at room temperature. The solid part was separated by centrifugation and dried, labeled as Ph-MIP@SiO₂. After phenol was eluted by 5% HCl, the surface imprinted polymer was then dried at 40 °C in a vacuum drying, labeled as MIP@SiO₂. For comparison, the non-imprinted polymer without phenol was prepared using the same method for MIP@SiO₂, labeled as NIP@SiO₂.

To remove SiO₂, the above prepared MIP@SiO₂ was etched in a hydrothermal reactor with 20mL of mixture of concentrated HF (40%) and HNO₃ (65%) solution (v/v 3:1) at 120 °C for 4 h, followed by centrifugation and wash with ultra-pure water for several times. The obtained product was dried at 60 °C by vacuum drying, labeled as MIP. The etching process of SiO₂ from Ph-MIP@SiO₂ and NIP@SiO₂ was the same, the corresponding products were labeled as Ph-MIP and NIP, respectively.

2.3 Fabrication of the surface MIECS

The as-received MWNTs were calcined in a tube furnace at 400 °C for 2 h to remove the residual catalysts and amorphous carbon particles before use³¹. The oxidation of MWNTs was carried on by reflux in a mixed solution of H₂SO₄ (98%) and HNO₃ (65%) with volume ratio of 3:1 at 80 °C for 4 h³²⁻³³. The carboxylic MWNTs was washed with ultrapure water for several times till neutral, separated by centrifugation at 9000 rpm for 15min and vacuum drying, labeled as MWNTs-COOH.

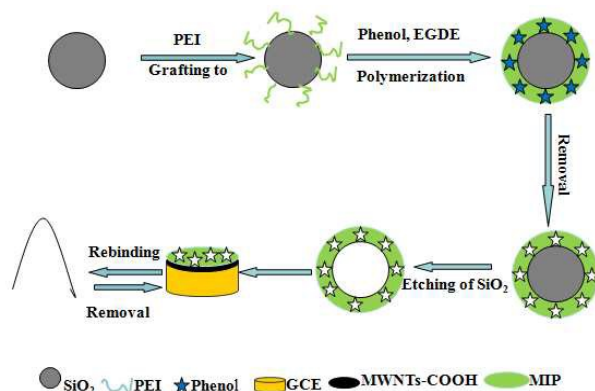
To get a mirror-like surface, a bare glass carbon electrode (GCE) was polished repeatedly using 0.05 μ m alumina aqueous slurry and rinsed, sonicated in ultrapure water and ethanol for 10 min, respectively. After being dried in air, 10 μ L of MWNTs-COOH suspension in DMF was dropped on the surface of GCE and dried under the infra-red light, the fabricated electrode was labeled as MWNTs-COOH/GCE. Finally, 10 μ L MIP suspension in DMF was

dropped on the formed MWNTs-COOH layer and dried again, the modified electrode was labeled as MIP/MWNTs-COOH/GCE. For comparison, Ph-MIP/MWNTs-COOH/GCE and NIP/MWNTs-COOH/GCE were prepared at the same conditions.

2.4 Physical Characterizations

Fourier transform infrared (FT-IR) spectra of the samples were characterized by a FTIR-8400 Infrared spectrometer (Bruker Tensor27, Rise China Electro-Optical Technology co., Ltd) with KBr disc method. The SEM images were recorded on a JEOL 6701F field emission scanning electron microscope (JEOL Co. Ltd).

The construction process of surface MIECS is depicted in Scheme 1.



Scheme 1 Schematic illustration of the fabrication process of the MIECS.

2.5 Electrochemical characterization and measurements

The cyclic voltammetry (CV) characterization was carried out on an Electrochemical Workstation (CHI660, Chenhua Company, Shanghai, China) with a three-electrode test system, in which the modified GCE was used as the working electrode, saturated calomel electrode (SCE) as the reference electrode and platinum wire as the counter electrode.

To determine the specific identification of the sensor, cyclic voltammograms (CVs) were recorded from -0.8V to 1.2V in 0.1M

phosphate buffer solutions (PBS, pH=7) containing phenol, the mixture of phenol and catechol, and the mixture of phenol, catechol and hydroquinone, respectively, with scan rate of 50mV/s. All the concentrations of phenol, catechol and hydroquinone were controlled as 1×10^{-6} M.

To test the sensitivity and determine the calibrate curve of the prepared sensor, differential pulse voltammetry (DPV) was recorded in 5 mM $K_3[Fe(CN)_6]$ solution containing phenol with different concentrations³⁴⁻³⁵. In our case, the measuring conditions were set as follows: the potential increment 4 mV, amplitude 50 mV, pulse width 50 ms³⁶⁻³⁷.

The reproducibility and stability of the sensor were examined by the following method: The used MIECS electrode was immersed into 5% HCl for 30 min to remove phenol and dried, and then the DPV of the reactivated sensor was recorded in the $K_3[Fe(CN)_6]$ solution containing 1×10^{-6} M phenol. The process was repeated for at least 10 times.

2.6 Real sample detection

To evaluate the analytical applicability of the prepared sensor, it was also applied to the determination of phenol in real samples such as tap water, river water (taken from Fenhe River) and treated coking wastewater (taken from local coking plant) using the standard addition method. Known amount of phenol (the concentrations were estimated to be 0.5 μ M and 1.0 μ M, respectively) was added into each sample before DPV measurement¹².

3. Results and Discussion

3.1 The elution of phenol from MIP

The detection performance of MIP electrochemical sensor strongly depends on the amount of cavities formed by removal of the template molecules³⁸. In this case, the more phenol being removed, the more imprinted cavities being formed. Fig.1 shows the CVs of Ph-MIP/MWNTs-COOH/GCE (a), MIP/MWNTs-COOH/GCE (b)

and NIP/MWNTs-COOH/GCE (c) in PBS solution with pH 7. Before the elution of phenol (Fig. 1a), the peak of the oxidation of phenol to benzoquinone³⁹ and the corresponding reduction peak during the negative scan are observed at 0.71 and 0.095 V, respectively. After the elution of the template molecules (Fig. 1b), the disappearance of the above characteristic peak demonstrates the successful removal of phenol from MIP. Fig. 1b and 1c are quite similar to each other, evidently shows the complete elution of phenol molecules from MIP by HCl solution. In addition, a couple of unobvious redox peaks at 0.15V (positive scan) and -0.35 V (negative scan) are also observed for all the three samples. We deduce that the peaks are attributed to the redox reaction of carboxyl group on the carbon nanotubes⁴⁰.

3.2 The etching of SiO₂ from MIP/SiO₂

Fig. 2 shows the FTIR spectra of SiO₂ (a), MIP@SiO₂ (b) and MIP after etching of SiO₂ (c). In comparison to the very strong adsorptions of pure SiO₂ (Fig. 2a) at 3446 cm⁻¹(Si-OH, v-as), 1103 cm⁻¹(Si-O-Si, v-as), 806 cm⁻¹(Si-O-Si, v-s), together with a relatively weak adsorption at 1638 cm⁻¹ (Si-OH, β)⁴¹, all the characteristic peaks of MIP@SiO₂ (Fig. 2b) weakened markedly because the surfaces of SiO₂ particles were covered by the MIP. Meanwhile, some new peaks are observed: the peak at 1643 cm⁻¹ contributes to the bending vibration of N-H, both of the peaks at 1568 and 1475 cm⁻¹ are assigned to the stretch vibration of C-N, indicating that MIP was successfully grafted to the surface of SiO₂. After the etching process, most of SiO₂ were removed, which could be proved by the sharp decrease of the characteristic peaks of SiO₂ (Fig. 2c)⁴²⁻⁴³.

Fig. 3(a), (b) and (c) show the morphologies of PEI@SiO₂, MIP@SiO₂ and MIP (etched by HF+HNO₃), respectively. The uneven surface observed for PEI@SiO₂ illustrates that PEI was grafted to SiO₂. With the imprint of phenol to PEI@SiO₂, the surface of MIP@SiO₂ became smooth due to the addition of cross-linking agent EGDE²⁴, leading to the fixed imprint sites over the surface.

After the etching process, the material softened and became smoother since SiO₂ was removed from MIP@SiO₂. However, some particles underneath the polymer layer are still faintly visible due to the incomplete removal of SiO₂, which is well consistent with the result obtained from the FTIR analysis.

3.3 The electrochemical performance of MIP/MWNTs-COOH/GCE

3.3.1 CV characterization

The cyclic voltammograms of the bare GCE, MIP@SiO₂/MWNTs-COOH /GCE, MIP/MWNTs-COOH /GCE and MWNTs-COOH /GCE in 0.1M KCl solution containing 5 mM K₃[Fe(CN)₆] are presented in Fig. 4a-d, respectively. In comparison with the CV of the bare GCE (Fig. 4a), the GCE electrode modified by MWNTs-COOH (Fig. 4d) shows much higher redox current of [Fe(CN)₆]³⁻/[Fe(CN)₆]⁴⁺, which could be attributed to the strong enhancement of MWNTs-COOH to the electron transfer of the electrode⁴⁴. For MIP@SiO₂/MWNTs-COOH /GCE (Fig. 4b), the redox current of [Fe(CN)₆]³⁻/[Fe(CN)₆]⁴⁺ sharply decreases due to the obstruction of electron transfer led by the non-conductive core of SiO₂ nanoparticles and the MIP matrix. After the removal of SiO₂ nanoparticles by etching, the redox current increases dramatically (MIP/MWNTs-COOH /GCE, Fig. 4c), though the current is still lower than that of MWNTs-COOH /GCE. It is interesting to mention that the holes generated by the elution of the template phenol facilitated the electron transfer of the sensor.

3.3.2 The specific recognition

For evaluating the specific recognition ability of the sensor, the CVs of MIP/MWNTs-COOH/GCE in PBS solution containing different phenolic compounds including pure phenol, the mixture of phenol and catechol, the mixture of phenol and hydroquinone, the mixture of phenol, hydroquinone and catechol were recorded

respectively, which are shown in Fig. 5(a-d). For comparison, the CV of MWNTs-COOH/GCE in phenol PBS solution (Fig. 5e) is presented as well. Obviously the CVs of MIP/MWNTs-COOH/GCE recorded in different phenolic solutions are quite similar, that is, only one peak at 0.86V corresponding to phenol oxidation is presented, indicating the specific recognition ability of MIP/MWNTs-COOH/GCE to phenol. The existence of other phenolic compounds showed no influence to the direct phenol detection. On the other hand, the CV curve of MWNTs-COOH/GCE in phenol PBS solution (Fig. 5e) shows three peaks: The strong oxidation peak of phenol at 0.71V is assigned to phenol oxidation to benzoquinone, indicating a higher activity of pure MWNTs-COOH compared to MIP/MWNTs-COOH. Nevertheless, two other peaks at 0.12 and 0.36 V are attributed to the oxidation of hydroquinone and catechol, respectively⁴⁵⁻⁴⁶, although neither hydroquinone or catechol was added into the test solution, which illustrates non-selectivity of pure MWNTs-COOH. This phenomenon further confirms the specific recognition ability of the fabricated MIECS to phenol.

However, the current intensities of the CVs directly obtained from phenol electro-oxidation are nearly half of those using $K_3[Fe(CN)_6]$ as active probe (as shown in Fig.4). On the other hand, the capacitive current in DPV is reduced in comparison to CV due to the different principles between the two test methods. In addition,

the sensitivity of phenol detection by CV might be reduced to some existence due to the inevitable interference of the intermediates, such as hydroquinone and catechol. Thus in the following research, the DPV responses of the active probe, $K_3[Fe(CN)_6]$, were measured to evaluate the properties of the fabricated sensor.

3.3.3 Calibration curve

Fig. 6 illustrates the DPV responses of MIP/MWNTs-COOH/GCE electrode in the aqueous solutions with different phenol concentration using $[Fe(CN)_6]^{3-}/[Fe(CN)_6]^{4-}$ as an electro-chemical active probe⁴⁷ (A) and the calibration curve of phenol (B). Obviously, the sharp and well-defined oxidation peak of $[Fe(CN)_6]^{3-}/[Fe(CN)_6]^{4-}$ weakens with the increase of the template molecule concentration (Fig. 6A), since the oxidation-reduction of $[Fe(CN)_6]^{3-}/[Fe(CN)_6]^{4-}$ was hindered gradually due to the occupation of imprinted cavities by phenol⁴⁸⁻⁴⁹. A linear relationship was fitted in the concentration range of $1 \times 10^{-8} \sim 1.8 \times 10^{-6}$ M with relation coefficient of 0.9942 (Fig. 6B). The detection limit of the sensor was calculated to be 4.2×10^{-9} M (S/N=3)⁵⁰, showing a larger linear range and lower detection limit compared to those of other electrochemical sensors reported in

Table 1 The performance comparison between the fabricated sensor and other electrochemical sensors reported in literature.

Methods	Modified materials	Linear range (M)	LOD(M)	References no.
SWV	ZnO/CNTs	$1.0 \times 10^{-6} - 7.5 \times 10^{-4}$	5×10^{-7}	51
i-t	enzyme/3D graphene	$5 \times 10^{-8} - 2 \times 10^{-6}$	5×10^{-8}	9
DPV	6B-PGE	$4 \times 10^{-5} - 3.2 \times 10^{-4}$	1.2×10^{-7}	52
CV	PDPA-MWCNT	$9.8 \times 10^{-6} - 8 \times 10^{-5}$	5×10^{-7}	53
SWV	2,7-BFCNPE/CNTs	$1 \times 10^{-5} - 9 \times 10^{-4}$	-	54
Biosensor	enzyme	-	7×10^{-6}	55
DPV	MIP/MWNTs	$1 \times 10^{-8} - 1.8 \times 10^{-6}$ M	1.4×10^{-9}	This work

Notes: SWV = Square wave voltammograms; i-t = Amperometric current-time curve; DAB = 3,3'-diaminobenzidine; PGE = Pencil graphite electrode; PDPA = Poly(Diphenylamine); 2,7-BFCNPE = 2,7-bis(ferrocenyl ethyl)fluoren-9-one

literatures^{9,51-55}, as listed in table 1. This could be contributed to not only the facilitated charge transfer process caused by the etching of SiO₂ nanoparticles and the modification of GCE with MWNTs-COOH, but also the recognition sites distributed on the surface of the polymer.

3.4 The reuseability and stability

The reuseability and stability of the sensor was studied by recording DPVs of the used MIP/MWNTs-COOH/GCE sensor in 5mM K₃[Fe(CN)₆] solution containing 1×10⁻⁶ M phenol after the elution of phenol. Fig. 7 shows the peak currents of phenol oxidation after repeated elution of phenol from the used sensor. It is clearly seen that the peak current barely changes, and the relative standard deviation (RSD) is 1.04% after repeat for 10 times. This demonstrates a good reuseability of the fabricated sensor. The current response to phenol of prepared sensor after long storage was tested as well to study the stability of the sensor. The modified electrode retains 98 % of its initial response after 20 days and 96 % after 40 days. The sensor exhibits good stability and can be used for the detection of phenol.

3.5 The phenol detection in real samples

The determination of phenol in the three real samples were

Table 2 Determination of phenol in real samples (n=3)

Samples	Phenol added (μM)	Peak current(μA)	Phenol found (μM)	Recovery (%)	RSD (%)
Tap water	0.5	118.0±0.01	0.49±0.01	97.54	0.8
	1	105.20±0.01	1.04±0.01	103.92	0.2
River water	0.5	117.40±0.02	0.51±0.07	102.72	1.2
	1	104.50±0.06	1.07±0.03	107.07	2.6
Treated waste water	0	121.20±0.02	0.35±0.07	-	1.8
	0.5	109.80±0.07	0.84±0.03	168.20	3.4
	1	97.98±0.04	1.35±0.02	135.04	1.4

carried out using the standard addition method and the corresponding results are listed in table 2. The results clearly show that the prepared MIP/MWCNT/GCE is a reliable and effective electrochemical sensor for phenol detection. Moreover, the interference from other species in water samples could be almost negligible.

4. Conclusions

In this work, a novel surface molecularly imprinted electrochemical sensor for phenol with specific recognition and high sensitivity was established. The sensor exhibited a remarkable enhancement of current response due to the facilitated charge transfer process caused by the etching of SiO₂ nanoparticles and the modification of GCE with MWNTs-COOH. In comparison to the other phenolic compounds, the sensor showed specific recognition to phenol together with excellent repeatability since the recognition site were distributed on the surface of the polymer. The linear range of the calibration curve was 1.00×10⁻⁸-1.80×10⁻⁶ M with the detection limit of 4.2×10⁻⁹ M (S/N=3) when potassium ferricyanide was used as the electro-chemical active probe. The fabricated sensor exhibited a good performance on the determination of phenol in real samples as well.

Acknowledgements

We wish to thank the financial support from the Natural Science Fund of Shanxi Province (Major project, No. 2014011003), the Research Project Supported by Shanxi Scholarship Council of China (No. 2012-006).

Notes and references

- S.-J. Yuan, J.-T. Gu, Y. Zheng, W. Jiang, B. Lianga and S.-O. Pehkonen, *Journal of Materials Chemistry A*, 2015, **3**, 4620-4636.
- P.-P. Qi, J.-C. Wang, L.-D. Wang, Y. Li, J. Jin, F. Su, Y.-J. Tian and J.-J. Chen, *Polymer*, 2010, **51**, 5417-5423.
- L. Shu, J.-K. Zhu, Q.-J. Wang, P.-G. He and Y.-Z. Fang, *Luminescence*, 2014, **29**, 579-585.
- B. Bukowska and S. Kowalska, *Toxicology Letters*, 2004, **152**, 73-84.
- X.-X. Han, L. Chen, U. Kuhlmann, C. Schulz, I. M. Weidinger and P. Hildebrandt, *Angewandte Chemie International Edition*, 2014, **53**, 2481-2484.
- T. Hofmann, E. Nebehaj and L. Albert, *Journal of Chromatography A*, 2015, **1393**, 96-105.
- Á. Kovács, M. Mörtl and A. Kende, *Microchemical Journal*, 2011, **99**, 125-131.
- A. V. Koliopoulos, D. K. Kampouris and C. E. Banks, *Analyst*, 2015, **140**, 3244-3250.
- F. Liu, Y.-X. Piao, J. S. Choi and T. S. Seo, *Biosensors Bioelectronics*, 2013, **50**, 387-392.
- Y.-X. Cheng, Y.-J. Liu, J.-J. Huang, K. Li, Y.-Z. Xian, W. Zhang and L.-T. Jin, *Electrochimica. Acta*, 2009, **54**, 2588-2594.
- B. J. Sanghavi and A. K. Srivastava, *Electrochimica. Acta*, 2011, **56**, 4188-4196.
- A. S. Ahammad, M. M. Rahman, G.-R. Xu, S. Kim and J.-J. Le, *Electrochimica. Acta*, 2011, **56**, 5266-5271.
- H.-H. Yang, S.-Q. Zhang, W. Yang, X.-L. Chen, Z.-X. Zhuang, J.-G. Xu and X.-R. Wang, *Journal of the American Chemical Society*, 2004, **126**, 4054-4055.
- L.-X. Chen, S.-F. Xu and J.-H. Li, *Chemical Society Reviews*, 2011, **40**, 2922-2942.
- M. P. Tiwari and A. P., *Analytica Chimica Acta*, 2015, **853**, 1-18.
- S. M. Reddy, G. Sette and Q. Phan, *Electrochimica. Acta*, 2011 **56**, 9203-9208.
- A. Bossi, F. Bonini, A.P.F. Turner and S.A. Piletsky, *Biosensors and Bioelectronics*, 2007, **22**, 1131-1137.
- L. Ye, K. Mosbach, *Chemistry of Materials*, 2008, **20**, 859-868.
- G. Wu, J.-Y. Li, X. Qu, Y.-X. Zhang, H. Hong and C.-S. Liu, *RSC Advances*, 2015, **5**, 4701-4702.
- B.-J. Gao, X.-J. Li, T. Chen and L. Fang, *Industrial and Engineering Chemistry Research*, 2014, **53**, 4469-4479.
- S. Banerjee and B. König, *Journal of the American Chemical Society*, 2013, **135**, 2967-2970.
- Q.-Y. Niu, K.-Z. Gao, Z.-H. Lin and W.-H. Wu, *Chemical Communications*, 2013, **49**, 9137-9139.
- B. B. Prasad, R. Madhuri, M. P. Tiwari and P. S. Sharma, *Electrochimica. Acta*, 2010, **55**, 9146-9156.
- P.-N. Zhao and J.-C. Hao, *Food Chemistry*, 2013, **139**, 1001-1007.
- L. Li, L.-L. Yang, Z.-L. Xing, X.-J. Lu and X.-W. Kan, *Analyst*, 2013, **138**, 6962-6968.
- H. Zhou, G.-L. Xu, A.-H. Zhu, Z. Zhao, C.-C. Ren, L.-L. Nie and X.-W. Kan, *RSC Advances*, 2012, **2**, 7803-7808.
- B.J. Gao, F.Q. An and Y. Zhu, *Polymer*, 2007, **48**, 2288-2297.
- B.J. Gao, F.Q. An, K.K. Liu, *Applied Surface Science*, 2006, **253**, 1946-1952.
- F.-Q. An, B.-J. Gao and X.-Q. Feng, *Journal of Hazardous Materials*, 2008, **157**, 286-292.
- A. Toyama, K. Ohta and H. Takeuchi, *Journal of Molecular Structure*, 2005, **735-736**, 235-241.
- X.-G. Sun and X.-S. Zeng, *New carbon materials*, 2004, **19**, 65-68.
- J.-M. You, D. Kim and S. Jeon, *Electrochimica. Acta*, 2012, **65**, 288-293.
- J.-Y. Kim, Y. Jo, S. Lee and H.-C. Choi, *Tetrahedron Letters*, 2009, **50**, 6290-6292.
- X.-Y. Zhang, Y. Peng, J.-L. Bai, B.-A. Ning, S.-M. Sun, X.-D. Hong, Y.-Y. Liu, Y. Liu and Z.-X. Gao, *Sensors and Actuators B*, 2014, **200**, 69-75.
- L. Li, L.-L. Yang, Z.-L. Xing, X.-J. Lu and X.-W. Kan, *Analyst*, 2013, **138**, 6962-6968.
- Q. Han, X. Wang, Z.-Y. Yang, W.-Y. Zhu, X.-M. Zhou and H.-J. Jiang, *Talanta*, 2014, **123**, 101-108.
- M. Chen, C.-F. Zhao, W. Chen, S.-H. Weng, A.-L. Liu, Q.-C. Liu, Z.-F. Zheng, J.-H. Lin and X.-H. Lin, *Analyst*, 2013, **138**, 7341-7346.
- M. P. Tiwari and A. Prasad, *Analytica Chimica Acta*, 2015, **853**, 1-18.
- Emma J. E. Stuart, M. Pumera, *Journal of Physical Chemistry. C* 2011, **115**, 5530-5534

ARTICLE

RSC Advances

- 40 Y. Shoja, A.-A. Rafati and J. Ghodsi, *Materials Science and Engineering C*, 2016, **58**, 835–845.
- 41 J. Fang, X.-F. Wang, L.-S. Wang, B. Cheng, Y.-T. Wu and W.-L. Zhu, *Chinese Science Bulletin*, 2007, **52**, 461-466.
- 42 F.-Q. An and B.-J. Gao, *Journal of Hazardous Materials*, 2008, **152**, 1186-1191.
- 43 B.-J. Gao, P.-F. Jiang, F.-Q. An, S.-Y. Zhao and Z. Ge, *Applied Surface Science*, 2005, **250**, 273–279.
- 44 C. Gao, Z. Guo, J.-H. Liu and X.-J. Huang, *Nanoscale*, 2012, **4**, 1948–1963.
- 45 S. N. Hussain, H. M. A. Asghar and A. K. Campen, *Electrochim. Acta*, 2013, **110**, 550-559.
- 46 L. Fang, F.-F. Li and G.-X. Zhang, *Chinese Science Bulletin*, 2015, **78**, 749-752.
- 47 B. Rezaei, M. K. Boroujeni and A. A. Ensafi, *Electrochimica Acta*, 2014, **123**, 332–339.
- 48 B. Rezaei, M.-K. Boroujeni and A.-A. Ensafi, *Biosensors and Bioelectronics*, 2014, **60**, 77–83.
- 49 H.-P. Bai, C.-Q. Wang, J. Chen, J. Peng and Q. Cao, *Biosensors and Bioelectronics*, 2015, **64**, 352–358.
- 50 M. L. Yola, T. Eren and N. Atar, *Biosensors and Bioelectronics*, 2014, **60**, 277–285.
- 51 K.-M. Hassan, M. Moazampour, A. -A. Ensafi, S. Mallakpour and M. Hatami, *Environment Science Polluted Research*, 2014, **21**, 5879–5888.
- 52 N. Vishnu and A.-S. Kumar, *Analyst. Methods* 2015, **7**, 1943–1950.
- 53 C.-Y. Yang, S.-M. Chen, T.-H. Tsai, B. Unnikrishnan, *International Journal of electrochemical science*, 2012, **7**, 12796-12807.
- 54 H.-M. Moghaddam, H. Beitollahi, S. Tajik, M. Malakootian and H.-K. Maleh, *Environmental Monitoring and Assessment*, 2014, **186**, 7431–7441.
- 55 R. Solna', S. Sapelnikova, P. Skla'dal, M. Winther-Nielsen, C. Carlsson, J. Emne'us and T. Ruzgas, *Talanta*, 2005, **65**, 349–357.

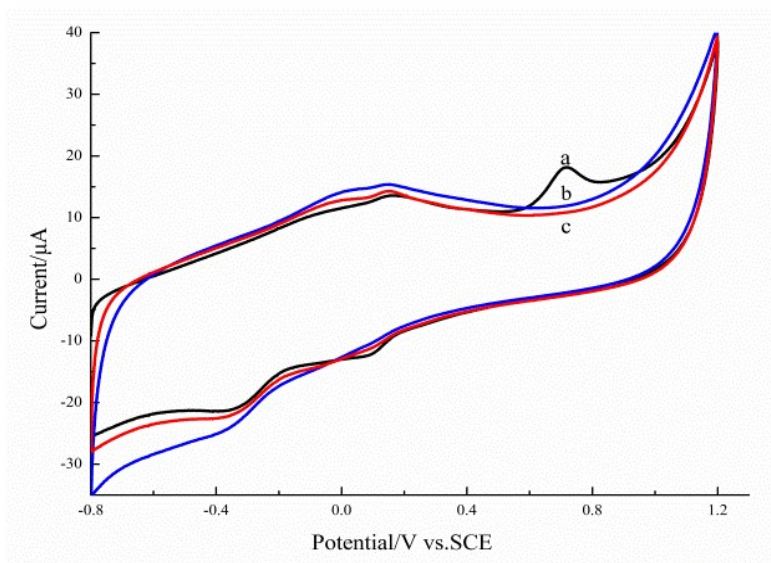


Fig. 1 CVs of Ph-MIP/MWNTs-COOH/GCE (a), MIP/MWNTs-COOH/GCE (b) and NIP/MWNTs-COOH/GCE (c) in 0.1M PBS (pH=7.0).

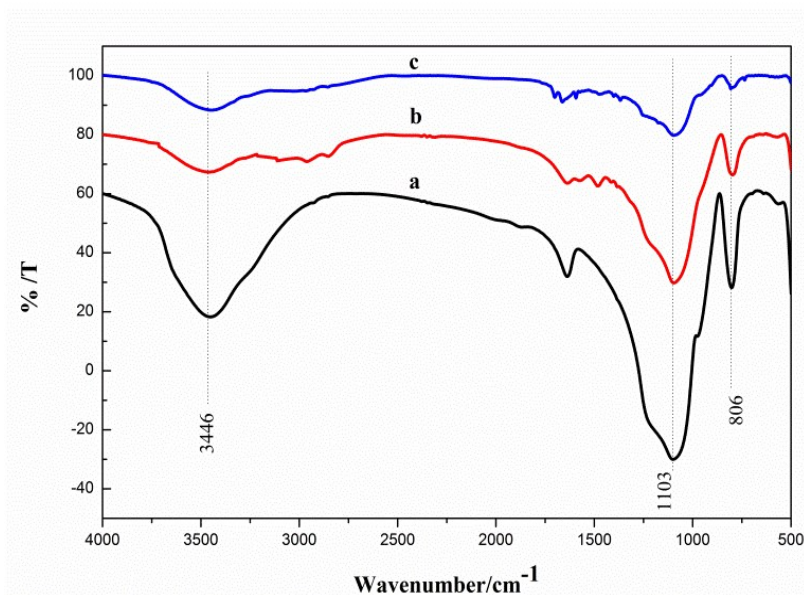


Fig. 2 FTIR spectra of SiO₂ (a), MIP@SiO₂ (b) and MIP after etching of SiO₂ (c).

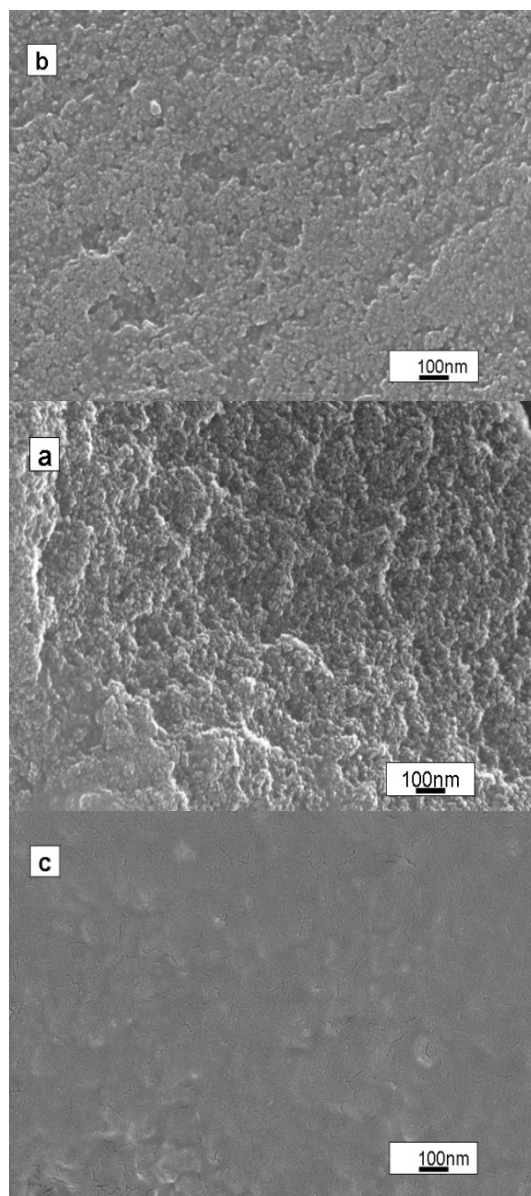


Fig.3 SEM images of (a) PEI@SiO₂, (b) MIP@SiO₂, (c) MIP@SiO₂ etched by HF+HNO₃.

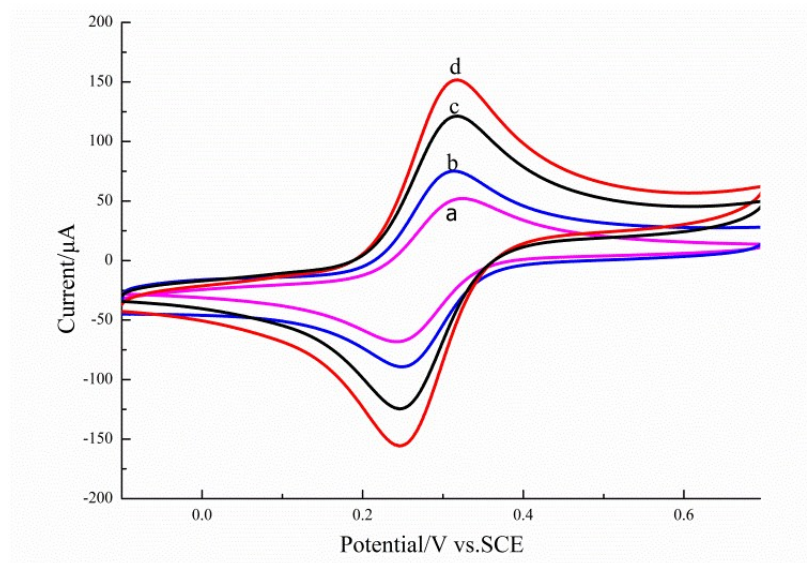


Fig. 4 CVs of the bare GCE electrode (a) and the modified electrodes in 0.1M KCl solution containing 5mM $K_3[Fe(CN)_6]$: MIP@SiO₂/MWNTs-COOH/GCE electrode (b), MIP/MWNTs-COOH /GCE electrode (c) and MWNTs-COOH /GCE electrode(d).

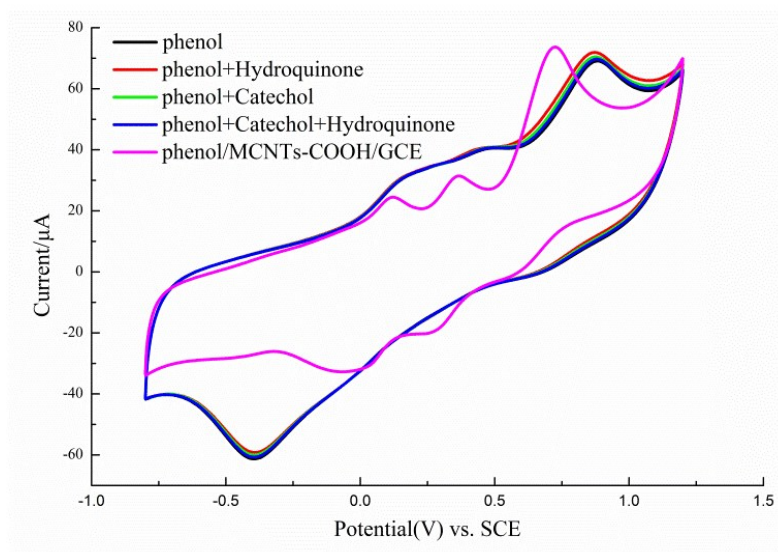


Fig. 5 CVs of MIP/MWNTs-COOH/GCE electrode in PBS (pH=7.0) containing phenol(a), phenol+hydroquinone(b), phenol+caechol (c), phenol+hideoquinone+catechol(d), and MWNTs-COOH/GCE in phenol(e), the concentrations of phenol in all the solutions were 1×10^{-6} M.

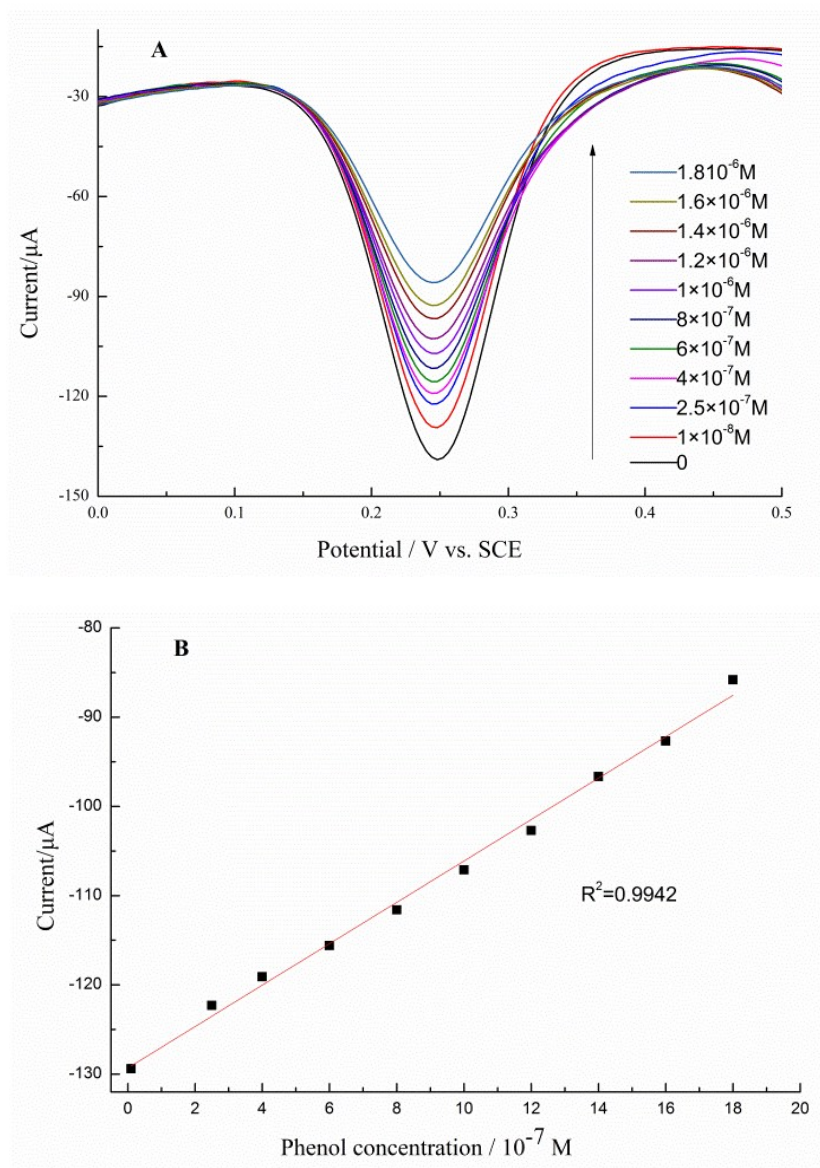


Fig. 6 (A) The DPVs of MIP/MWNTs-COOH/GCE in the aqueous solutions containing 0.1 M KCl, 5 mM $[\text{Fe}(\text{CN})_6]^{3-}/[\text{Fe}(\text{CN})_6]^{4-}$, and phenol (the arrow direction is from 1×10^{-8} to 1.8×10^{-6} M); (B) The calibration curve of phenol.

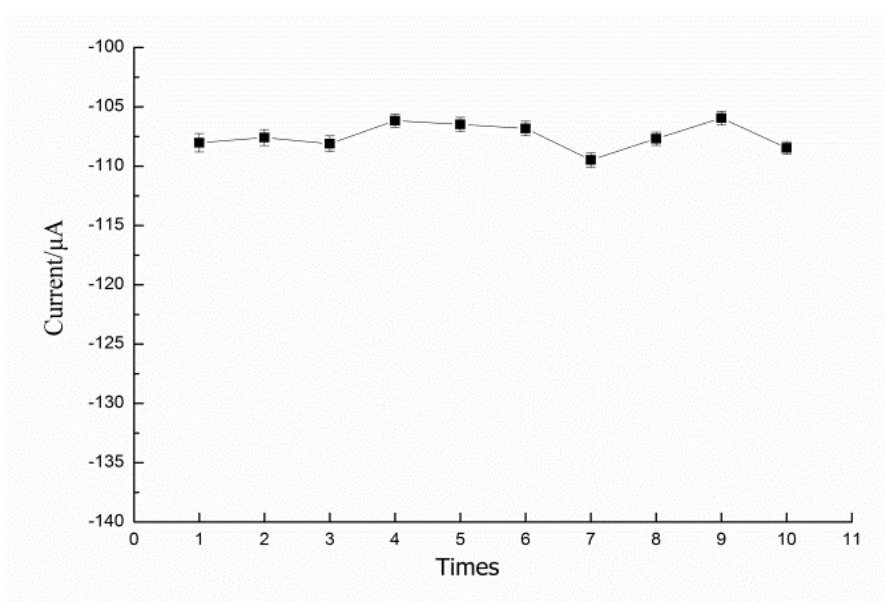
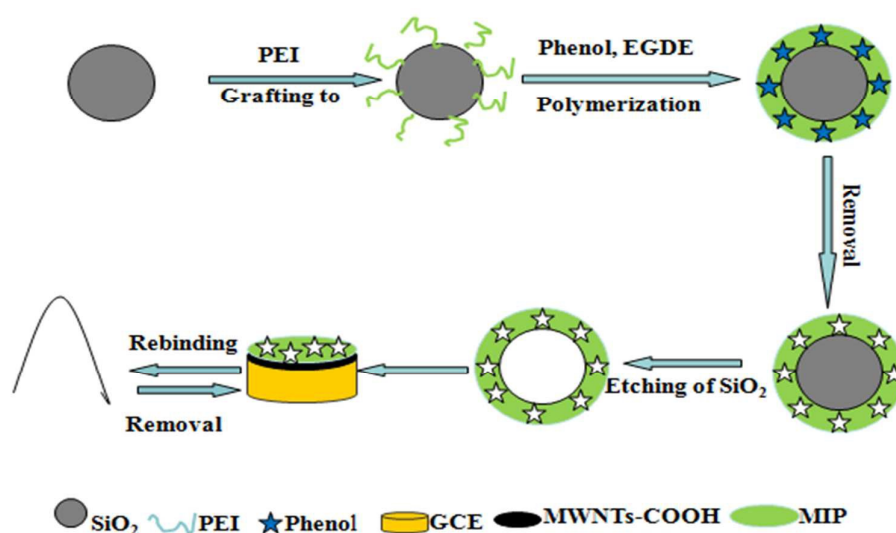


Fig. 7 The reusability of MIP/MWCNT/GCE. (test solution: 0.1 M KCl solution containing 5mM $K_3[Fe(CN)_6]$ and 1×10^{-6} M phenol).

Graphical abstract

In this paper, A novel surface molecularly imprinted electrochemical sensor (MIECS) for recognition and detection of phenol was constructed by dispersing a molecularly imprinted polymer (MIP) film on a multi-walled carbon nanotubes (MWNTs) modified glass carbon electrode (GCE). An adsorption equilibrium of phenol to polyethyleneimine (PEI, grafted to SiO₂ nanoparticles) had been achieved before molecular imprinting was carried out towards PEI by using phenol as a template and ethylene glycol diglycidyl ether (EGDE) as cross-linker. The MIP was fabricated after the removal of phenol and the etching of SiO₂ nanoparticles. The obtained MIECS were characterized by cyclic voltammetry (CV) and differential pulse voltammetry (DPV). The linear range of the calibration curve was 1×10^{-8} - 1.8×10^{-6} M with the detection limit of 4.2×10^{-9} M (S/N=3) when potassium ferricyanide was used as electro-chemical active probe.



Scheme 1. Schematic illustration of the fabrication process of the MIECS.